

# Acceleration statistics of heavy particles in turbulence

By **J. BEC<sup>1</sup>, L. BIFERALE<sup>2</sup>, G. BOFFETTA<sup>3</sup>,  
A. CELANI<sup>4</sup>, M. CENCINI<sup>5</sup>, A. LANOTTE<sup>6</sup>,  
S. MUSACCHIO<sup>7</sup>, AND F. TOSCHI<sup>8</sup>**

<sup>1</sup> CNRS Observatoire de la Côte d'Azur, B.P. 4229, 06304 Nice Cedex 4, France

<sup>2</sup> Dept. of Physics and INFN, University of Rome "Tor Vergata",  
Via della Ricerca Scientifica 1, 00133 Roma, Italy

<sup>3</sup> Dept. of Physics and INFN, University of Torino, Via Pietro Giuria 1, 10125, Torino, Italy

<sup>4</sup> CNRS, INLN, 1361 Route des Lucioles, F-06560 Valbonne, France.

<sup>5</sup> SMC-INFN c/o Dept. of Physics University of Rome "La Sapienza", Piazz.le A. Moro, 2,  
I-00185 Roma, Italy, and CNR-ISC via dei Taurini, 19 I-00185 Roma, Italy.

<sup>6</sup> CNR-ISAC, Sezione di Lecce, Str. Prov. Lecce-Monteroni km.1200, I-73100 Lecce, Italy

<sup>7</sup> Dept. of Physics, University of Rome "La Sapienza", Piazz.le A. Moro, 2, I-00185 Roma, Italy

<sup>8</sup> CNR-IAC, Viale del Policlinico 137, I-00161 Roma, Italy and  
INFN, Sezione di Ferrara, via G. Saragat 1, I-44100, Ferrara, Italy.

(Received 24 May 2019)

We present the results of direct numerical simulations of heavy particle transport in homogeneous, isotropic, fully developed turbulence, up to resolution  $512^3$  ( $R_\lambda \approx 185$ ). Following the trajectories of up to 120 million particles with Stokes numbers,  $St$ , in the range from 0.16 to 3.5 we are able to characterize in full detail the statistics of particle acceleration. We show that: (i) The root-mean-squared acceleration  $a_{\text{rms}}$  sharply falls off from the fluid tracer value already at quite small Stokes numbers; (ii) At a given  $St$  the normalised acceleration  $a_{\text{rms}}/(\epsilon^3/\nu)^{1/4}$  increases with  $R_\lambda$  consistently with the trend observed for fluid tracers; (iii) The tails of the probability density function of the normalised acceleration  $a/a_{\text{rms}}$  decrease with  $St$ . Two concurrent mechanisms lead to the above results: particle clustering, very effective at small  $St$ , and filtering induced by the particle response time, that takes over at larger  $St$ .

## 1. Introduction

Small impurities like dust, droplets or bubbles suspended in an incompressible flow are finite-size particles whose density may differ from that of the underlying fluid, and cannot thus be modelled as point-like tracers. The description of their motion must account for inertia whence the name *inertial particles*. At long times particles concentrate on singular sets evolving with the fluid motion, leading to the apparition of a strong spatial inhomogeneity dubbed *preferential concentration* (see e.g. Fig. 1). At the experimental level such inhomogeneities have been long known (see Eaton & Fessler 1994 for a review) and utilised for flow visualisation (e.g. exploiting bubble clustering inside vortex filaments). The statistical description of particle concentration is at present a largely open question with many industrial and environmental applications. We mention spray combustion in Diesel engines (Post & Abraham 2002) or some rocket propellers (Pinsky & Khain 1997), the formation of rain droplets in warm clouds (Falkovich, Fouxon & Stepanov 2002, Shaw 2003)

or the coexistence of plankton species (Rothschild & Osborn 1988, Lewis & Pedley 2000). Inertial particles are also relevant to spore, pollen, dust or chemicals dispersion in the atmosphere where the diffusion by air turbulence may be even overcome by preferential clustering (Csanady 1980, Seinfeld 1986).

From the experimental side, the study of particle motion in turbulence has recently undergone rapid progress thanks to the development of effective optical and acoustical tracking techniques (La Porta *et al.* 2001, La Porta *et al.* 2002, Mordant *et al.* 2001, Warhaft, Gylfason, & Ayyalasomayajula 2005). In parallel with experimental effort, theoretical analysis (Balkovsky, Falkovich & Fouxon 2001, Falkovich & Pumir 2004, Bec, Gawedzki & Horvai 2004, Zaichik, Simonin & Alipchenkov 2003) and numerical simulations (Boivin, Simonin, Squires 1998, Reade & Collins 2000, Zhou, Wexler & Wang 2001, Chun *et al.* 2005) are paving the way to a thorough understanding of inertial particle dynamics in turbulent flows. Recently, the presence of strong inhomogeneities characterised by fractal and multifractal properties have been predicted, and found in theoretical and numerical studies of stochastic laminar flows (Balkovsky, Falkovich & Fouxon 2001, Bec, Gawedzki & Horvai 2004, Bec 2003), in two dimensional turbulent flows (Boffetta, De Lillo & Gamba 2004) and in three dimensional turbulent flows at moderate Reynolds numbers in the limit of vanishing inertia (Falkovich & Pumir 2004).

Here we present a Direct Numerical Simulations (DNS) study of particles much heavier than the carrier fluid in high-resolution turbulent flows. In particular, we shall focus on the behaviour of particle acceleration at varying both Stokes and Reynolds numbers. For fluid tracers, it is known that trapping into vortex filaments (La Porta *et al.* 2001, Biferale *et al.* 2005) is the main source of strong acceleration events. On the other hand, little is known about the acceleration statistics of heavy particles in turbulent flows, where preferential concentration may play a crucial role. Moreover, since in most applied cases it is almost impossible to perform DNS of particle transport in realistic settings, it is very important to understand acceleration statistics for building stochastic models of particle motion with and without inertia (Sawford & Guest 1991).

The material is organised as follows. In § 2, we briefly recall the equations of motion of the inertial particles and summarise the DNS set up. In § 3, we present and discuss the main results concerning the acceleration statistics. The final Section is devoted to conclusions and perspectives.

## 2. Heavy particle dynamics and numerical simulations

The equations of motion of a small, rigid, spherical particle immersed in an incompressible flow have been consistently derived from first principles by Maxey & Riley 1983. In the limiting case of particles much heavier than the surrounding fluid, these equations take the particularly simple form

$$\frac{d\mathbf{X}}{dt} = \mathbf{V}(t), \quad \frac{d\mathbf{V}}{dt} = -\frac{\mathbf{V}(t) - \mathbf{u}(\mathbf{X}(t), t)}{\tau_s}. \quad (2.1)$$

Here,  $\mathbf{X}(t)$  denotes the particle trajectory,  $\mathbf{V}(t)$  its velocity,  $\mathbf{u}(\mathbf{x}, t)$  is the fluid velocity. The Stokes response time is  $\tau_s = 2\rho_p a^2 / (9\rho_f \nu)$  where  $a$  is the particle radius  $\rho_p$  and  $\rho_f$  are the particle and fluid density, respectively, and  $\nu$  is the fluid kinematical viscosity. The Stokes number is defined as  $St = \tau_s / \tau_\eta$  where  $\tau_\eta = (\nu/\epsilon)^{1/2}$  is the Kolmogorov timescale and  $\epsilon$  the average rate of energy injection. Eq. (2.1) is valid for very dilute suspensions, where particle-particle interactions (collisions) and hydrodynamic coupling are not taken into account.

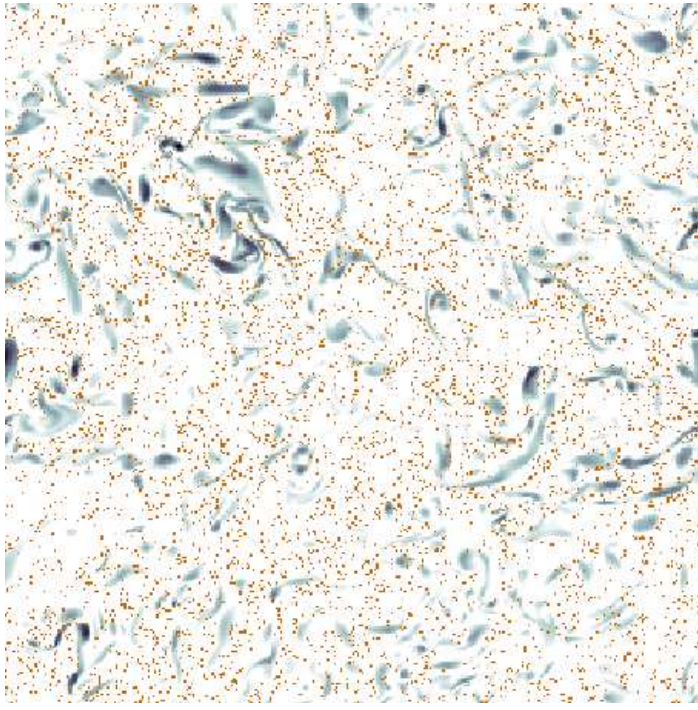


FIGURE 1. Snapshot of particle positions in a plane for small Stokes number,  $St = 0.16$ . The greyscale codes the modulus of the vorticity field. Notice that particles escape from high vorticity regions. For a quantitative measurement of the small scale clustering see the inset of Fig. 2a.

The fluid evolves according to the incompressible Navier-Stokes equations

$$\frac{\partial \mathbf{u}}{\partial t} + \mathbf{u} \cdot \nabla \mathbf{u} = -\frac{\nabla p}{\rho_f} + \nu \Delta \mathbf{u} + \mathbf{f}, \quad (2.2)$$

where  $p$  is the pressure field and  $\mathbf{f}$  is the external energy source,  $\langle \mathbf{f} \cdot \mathbf{u} \rangle = \epsilon$ .

The Navier-Stokes equations are solved on a cubic grid of size  $N^3$  for  $N = 128, 256, 512$  with periodic boundary conditions. Energy is injected by keeping constant the spectral content of the two smallest wavenumber shells (Chen *et al.* 1993). The viscosity is chosen so to have a Kolmogorov lengthscale  $\eta \approx \Delta x$  where  $\Delta x$  is the grid spacing: this choice ensures a good resolution of the small-scale velocity dynamics. We use a fully dealiased pseudospectral algorithm with 2<sup>nd</sup> order Adam-Bashforth time-stepping. The Reynolds numbers achieved are in the range  $R_\lambda \in [65 : 185]$ .

The equations of fluid motion are integrated until the system reaches a statistically steady state. Then, particles are seeded with homogeneously distributed initial positions and velocities equal to the local fluid velocity. Equations (2.1) and (2.2) are then advanced in parallel. A transient in particle dynamics follows, about 2–3 large scale eddy turn over time, before reaching a Lagrangian stationary statistics. It is only after this relaxation stage has completely elapsed that the real measurement starts. We followed 15 sets of inertial particles with Stokes numbers from 0.16 to 3.5. For each set, we saved the position and the velocity of  $N_t$  particles every  $dt = 1/10\tau_\eta$  with a maximum number of recorded trajectories of  $N_t = 5 \cdot 10^5$  for the highest resolution. Along these trajectories we also stored the velocity of the carrier fluid. At a lower frequency  $\sim 10\tau_\eta$ , we saved the positions and velocities of a larger number  $N_p$  of particles (up to  $7.5 \cdot 10^6$  per  $St$  at the highest resolution) together with the Eulerian velocity field. We have also followed fluid tracers

$R_\lambda$	$u_{\text{rms}}$	$\varepsilon$	$\nu$	$\eta$	$L$	$T_E$	$\tau_\eta$	$T_{\text{tot}}$	$T_{\text{tr}}$	$\Delta x$	$N^3$	$N_t$	$N_p$	$N_{\text{tot}}$
185	1.4	0.94	0.00205	0.010	$\pi$	2.2	0.047	14	4	0.012	$512^3$	$5 \cdot 10^5$	$7.5 \cdot 10^6$	$12 \cdot 10^7$
105	1.4	0.93	0.00502	0.020	$\pi$	2.2	0.073	20	4	0.024	$256^3$	$2.5 \cdot 10^5$	$2 \cdot 10^6$	$32 \cdot 10^6$
65	1.4	0.85	0.01	0.034	$\pi$	2.2	0.110	29	6	0.048	$128^3$	$3.1 \cdot 10^4$	$2.5 \cdot 10^5$	$4 \cdot 10^6$

TABLE 1. Parameters of DNS. Microscale Reynolds number  $R_\lambda$ , root-mean-square velocity  $u_{\text{rms}}$ , energy dissipation  $\varepsilon$ , viscosity  $\nu$ , Kolmogorov lengthscale  $\eta = (\nu^3/\varepsilon)^{1/4}$ , integral scale  $L$ , large-eddy Eulerian turnover time  $T_E = L/u_{\text{rms}}$ , Kolmogorov timescale  $\tau_\eta$ , total integration time  $T_{\text{tot}}$ , duration of the transient regime  $T_{\text{tr}}$ , grid spacing  $\Delta x$ , resolution  $N^3$ , number of trajectories of inertial particles for each Stokes  $N_t$  saved at frequency  $\tau_\eta/10$ , number of particles  $N_p$  per Stokes stored at frequency  $10\tau_\eta$ , total number of advected particles  $N_{\text{tot}}$ . Errors on all statistically fluctuating quantities are of the order of 10%.

( $St = 0$ ), that evolve according to the dynamics

$$\frac{d\mathbf{x}(t)}{dt} = \mathbf{u}(\mathbf{x}(t), t), \quad (2.3)$$

in order to systematically assess the importance of the phenomenon of preferential concentration at varying both  $St$  and  $R_\lambda$ .

A summary of the various physical parameters is given in table 1.

### 3. Results and discussion

In this paper we focus on the statistics of particle acceleration  $\mathbf{a}(t) = \frac{d\mathbf{V}}{dt}$ . From previous studies on fluid tracers we know that acceleration statistics is very intermittent and strong fluctuations are associated to trapping events within vortical filaments (La Porta *et al.* 2001, La Porta *et al.* 2002, Mordant *et al.* 2001, Biferale *et al.* 2005). How does inertia impacts acceleration statistics? A good starting point to gain insight on the effect of inertia is given by the formal solution of Eqs. (2.1) in the statistically stationary state, relating the instantaneous particle velocity to the previous history of fluid velocity along the particle trajectory. The expression is

$$\mathbf{V}(t) = \int_{-\infty}^t e^{-(t-s)/\tau_s} \mathbf{u}(\mathbf{X}(s), s) ds \quad (3.1)$$

yielding for the acceleration

$$\mathbf{a}(t) = \tau_s^{-1} \int_{-\infty}^t e^{-(t-s)/\tau_s} [\mathbf{u}(\mathbf{X}(t), t) - \mathbf{u}(\mathbf{X}(s), s)] ds. \quad (3.2)$$

It is instructive to analyse separately the two limiting cases of small and large Stokes numbers.

At small  $St$ , i.e.  $\tau_s \ll \tau_\eta$ , the fluid velocity along the trajectory evolves smoothly in time and the above expression for the acceleration reduces to  $\mathbf{a}(t) \simeq \frac{d}{dt} \mathbf{u}(\mathbf{X}(t), t)$ , i.e. to the derivative of fluid velocity along the inertial particle trajectory. At sufficiently small  $St$  this is indistinguishable from the fluid acceleration  $\frac{D\mathbf{u}}{Dt}(\mathbf{X}(t), t)$  evaluated at particle positions. The latter, in turn, is essentially dominated by the  $-\nabla p$  contribution. Therefore we are led to draw the following picture for the small  $St$  case: the heavy particle acceleration essentially coincides with the fluid acceleration; however, inertial particles are not homogeneously distributed in the flow and concentrate preferentially inside regions with relatively small pressure gradient (low vorticity regions – see Fig.

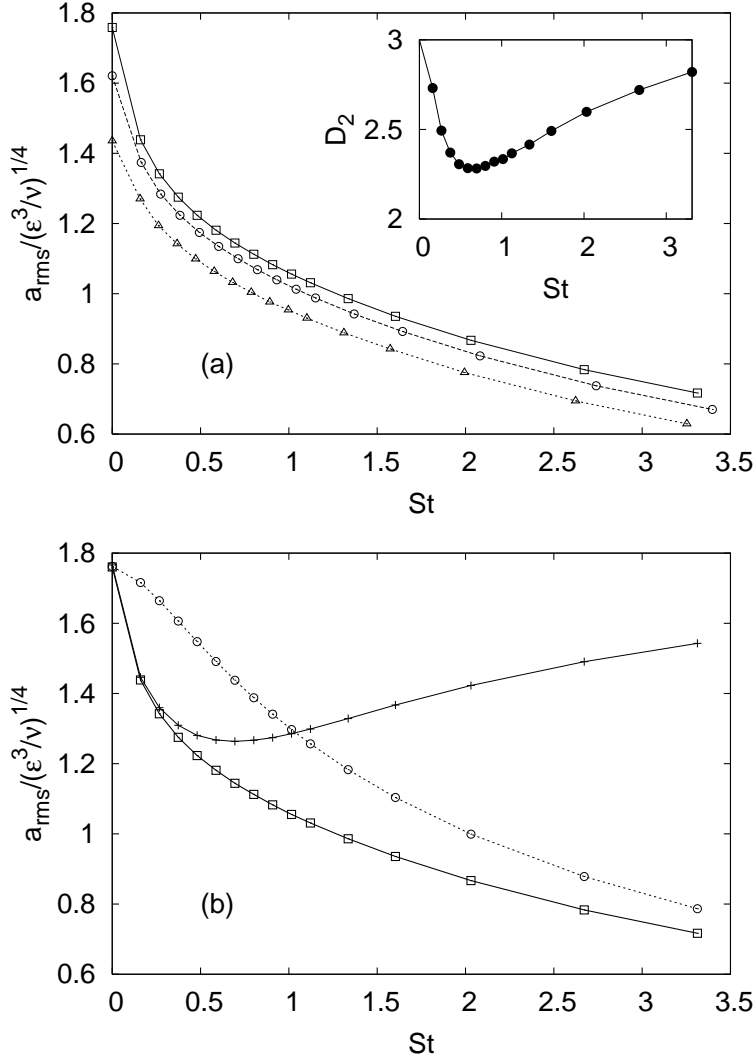


FIGURE 2. (a) The normalised acceleration variance  $a_{\text{rms}}/(\varepsilon^3/\nu)^{1/4}$  as a function of the Stokes number for  $R_\lambda = 185$  ( $\square$ );  $R_\lambda = 105$  ( $\circ$ );  $R_\lambda = 65$  ( $\triangle$ ). The inhomogeneous distribution of particle is quantified for the highest Reynolds in the inset, where we plot the correlation dimension,  $D_2$ , as a function of  $St$ . The correlation dimension is defined as  $p(r) \sim r^{D_2}$  (for  $r \ll \eta$ ) where  $p(r)$  is the probability to find two particles at distance smaller than  $r$  (Bec *et al.* 2005). (b) Comparison between the acceleration variance,  $a_{\text{rms}}$  ( $\square$ ), as a function of Stokes, with the acceleration of the fluid tracer measured on the particle position,  $\langle (\frac{D\mathbf{u}}{Dt})^2 \rangle^{1/2}$  (+). The last curve ( $\circ$ ), approaching the  $a_{\text{rms}}$  for large  $St$ , is the one obtained from the filtered tracer trajectories,  $a_{\text{rms}}^F$ . All data refer to  $Re_\lambda = 185$ .

1). As a result, the net effect of inertia is a drastic reduction of the root-mean-squared acceleration  $a_{\text{rms}} = \langle \mathbf{a}^2 \rangle^{1/2}$ , due essentially to particle clustering. Indeed, as shown in Fig. 2a the acceleration variance drops off very fast already at quite small  $St$  values. In Fig. 2b we give evidence that the value of  $a_{\text{rms}}$  is very close for  $St < 0.4$  to  $\langle (\frac{D\mathbf{u}}{Dt})^2 \rangle^{1/2}$  when the average is not taken homogeneously in space but conditioned to be on the same spatial positions of the inertial particles. The agreement of the two curves supports the

arguments above. Notice that at increasing Stokes the two curves start to deviate from each other, the tracer acceleration conditioned on the particle positions has a minimum for  $St \approx 0.5$  close to the maximum of clusterisation (see inset of Fig. 2a), eventually recovering the value of  $a_{\text{rms}}$  of the unconditioned tracers for larger  $St$ . The latter effect is a clear indication that inertial particles explore the small scale structures of the flow more and more homogeneously by increasing  $St$ . In this limit a different mechanism is responsible for the reduction of the  $a_{\text{rms}}$ .

At large  $St$ , i.e.  $\tau_s \gg \tau_\eta$ , the inspection of Eq. (3.2) shows that the main effect of inertia on particle acceleration is a low-pass filtering of fluid velocity differences, with a suppression of fast frequencies above  $\tau_s^{-1}$ . In figure 1b we also compare the acceleration variance with the one obtained by an artificial low-pass filtering based only on the fluid tracers trajectories. For each tracer trajectory,  $\mathbf{x}(t)$ , we define a new velocity,  $\mathbf{u}^F$ , filtered on a window-size of the same order of the Stokes time:

$$\mathbf{u}^F(t) = \int_{-\infty}^t e^{-(t-s)/\tau_s} \mathbf{u}(\mathbf{x}(s), s) ds \quad (3.3)$$

The filtered acceleration is thus given by  $\mathbf{a}^F = \frac{d}{dt} \mathbf{u}^F$ . The root mean square fluctuation,  $a_{\text{rms}}^F = \langle (\frac{d}{dt} \mathbf{u}^F)^2 \rangle^{1/2}$ , is computed by averaging along the tracer trajectories without any condition on their spatial positions, i.e. homogeneously distributed in the whole 3d domain. The curves corresponding to  $a_{\text{rms}}$  and to  $a_{\text{rms}}^F$  tend to approach as  $St$  grows larger, supporting the conjecture that preferential concentration for  $St > 1$  becomes less important. For intermediate  $St$  we expect a non trivial interplay between the two above mechanisms that makes very difficult to build up a model able to reproduce even the qualitative behaviour.

Another interesting aspect shown in Fig. 2a is the residual dependence of the normalised particle acceleration on Reynolds number. For the case of fluid tracers it is known that intermittent corrections to the dimensional estimate  $a_{\text{rms}} = a_0(\epsilon^3/\nu)^{1/2}$  may explain the Reynolds dependence (Sawford *et al.* 2003, Hill 2002, Biferale *et al.* 2004). Data suggest that the fluid intermittency may be responsible of such deviations at  $St > 0$  as well. This view is supported by the fact that the curves for the three Reynolds numbers are almost parallel.

A two-parameters formula for the variance of the acceleration as a function of Stokes number can be derived in the limit of vanishing Stokes numbers as:  $a_{\text{rms}}^2(St) = a_{\text{rms}}^2(0) + C \exp[-(D/St)^\delta]$  (Falkovich 2005). This expression follows from the acceleration pdf of tracer particles under the assumptions that (i) the main effect of inertia is to reduce the particle concentration in regions where the accelerations is larger than  $\nu^{1/2}/\tau_s^{3/2}$ ; (ii) the pdf tail is well reproduced by a stretched exponential shape with exponent  $\beta = 2/3\delta$ . Although the formula fits well the data, the limitation of our data-set to only a few points with  $St \ll 1$  does not permit a significant benchmark of the model.

In table 2 we summarise the values that we have measured for  $\langle \mathbf{a}^2 \rangle$  and  $\langle \mathbf{a}^4 \rangle$  as a function of all Stokes and for all Reynolds numbers available.

Besides the effect of inertia on typical particle accelerations it is also interesting to investigate the effects on the form of the probability distribution function  $\mathbf{a}(t)$ . As shown in Fig. 3a, the pdf's get less and less intermittent as  $St$  increases. In the inset of the same figure we show the behaviour of the flatness,  $\langle \mathbf{a}^4 \rangle / \langle \mathbf{a}^2 \rangle^2$ , as a function of  $St$ . The abrupt decreasing for  $St > 0$  is even more evident here (notice that the  $y$  scale is logarithmic). In the limits of small and large  $St$  the qualitative trend of the pdf's can be captured by the same arguments used for  $a_{\text{rms}}$ . In Fig. 3b we compare the pdf shape for the smallest Stokes number with the one obtained by using the tracer acceleration measured on the

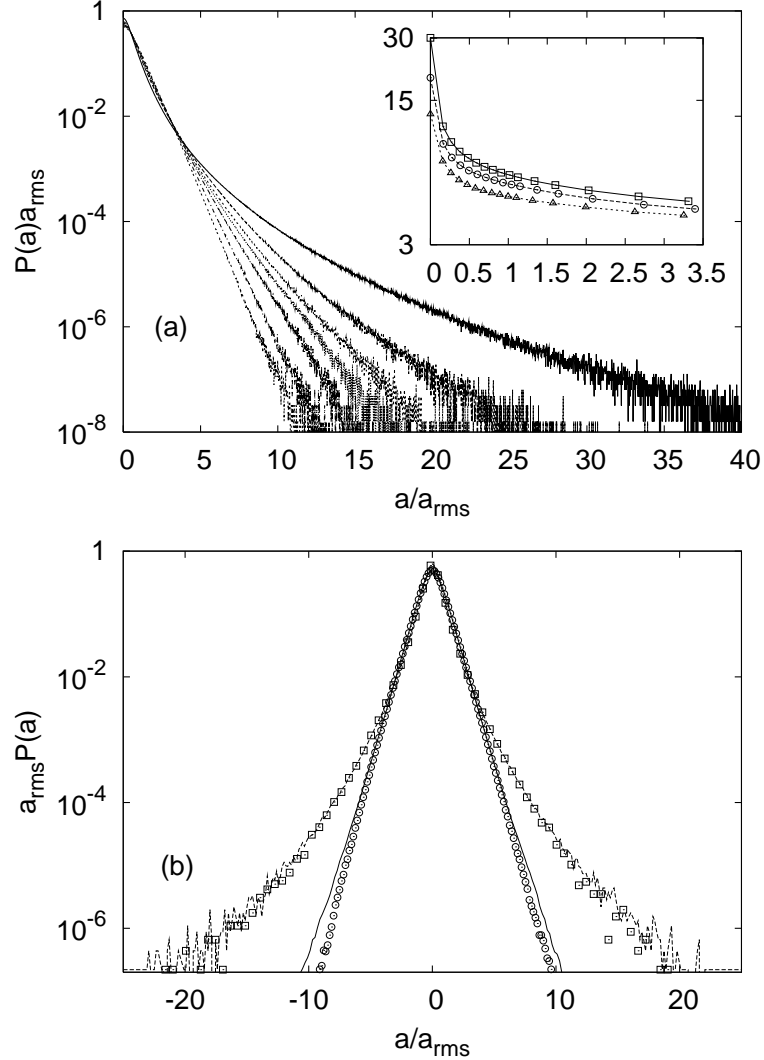


FIGURE 3. (a) Acceleration pdf's for a subset of Stokes values ( $St = 0, 0.16, 0.37, 0.58, 1.01, 2.03, 3.31$  from top to bottom) at  $R_\lambda = 185$ . The inset displays the acceleration flatness,  $\langle a^4 \rangle / \langle a^2 \rangle^2$ , at increasing  $R_\lambda$  from bottom to top. (b) The two more external curves correspond to the acceleration pdf for  $St = 0.16$  ( $\square$ ) and the pdf of the fluid tracers acceleration measured on the same position of the inertial particles,  $\frac{D\mathbf{u}}{Dt}$  (solid line). The two inner curves are the acceleration pdf at the highest Stokes,  $St = 3.31$ , ( $\circ$ ) and the pdf of the filtered fluid acceleration (solid line). All curves are normalised to have unit variance.

particle position,  $\frac{D\mathbf{u}}{Dt}$ . As one can see the two functions overlap perfectly, confirming that the only difference between fluid particles and inertia particles for small Stokes is due to preferential concentration. In the same figure we also compare for the highest Stokes,  $St = 3.31$ , the pdf of the particle acceleration with the one obtained from the filtered fluid trajectories. Now the agreement is less perfect but still fairly good, reassuring that this limit can be captured starting from a low-pass filter of fluid tracer velocities.

St <sup>(a)</sup>	0	0.16	0.27	0.37	0.48	0.59	0.69	0.80	0.91	1.01	1.12	1.34	1.60	2.03	2.67	3.31
$\langle \tilde{a}^2 \rangle$	3.09	2.07	1.80	1.63	1.50	1.39	1.31	1.24	1.17	1.12	1.06	0.97	0.88	0.75	0.61	0.51
$\langle \tilde{a}^4 \rangle$	288	48.1	30.5	22.4	17.7	14.5	12.3	10.6	9.20	8.11	7.21	5.77	4.47	3.11	1.94	1.29
St <sup>(b)</sup>	0	0.16	0.27	0.38	0.49	0.60	0.71	0.82	0.93	1.04	1.15	1.37	1.64	2.08	2.74	3.40
$\langle \tilde{a}^2 \rangle$	2.63	1.89	1.65	1.45	1.38	1.29	1.21	1.14	1.08	1.03	0.98	0.89	0.80	0.68	0.54	0.45
$\langle \tilde{a}^4 \rangle$	133	32.9	21.6	16.3	13.1	10.9	9.29	8.03	7.01	6.18	5.48	4.37	3.36	2.23	1.39	0.90
St <sup>(c)</sup>	0	0.16	0.26	0.37	0.47	0.58	0.68	0.79	0.89	1.00	1.10	1.31	1.57	1.99	2.62	3.25
$\langle \tilde{a}^2 \rangle$	2.02	1.59	1.40	1.28	1.19	1.11	1.05	0.99	0.94	0.89	0.85	0.77	0.70	0.59	0.47	0.39
$\langle \tilde{a}^4 \rangle$	52.8	19.1	13.1	10.1	8.24	6.95	6.01	5.24	4.61	4.11	3.67	2.95	2.32	1.59	0.97	0.63

TABLE 2. Normalised values of the second and fourth moments of the acceleration  $\langle \tilde{a}^2 \rangle = \langle \tilde{a}^2 \rangle / [3(\epsilon^3/\nu)^{1/2}]$ ,  $\langle \tilde{a}^4 \rangle = \langle \tilde{a}^4 \rangle / [3(\epsilon^3/\nu)]$  for <sup>(a)</sup>  $R_\lambda = 185$ , <sup>(b)</sup>  $R_\lambda = 105$  and <sup>(c)</sup>  $R_\lambda = 65$ . The statistical error on all entries are of the order of 5%.

#### 4. Conclusions and perspectives

A systematic study of the acceleration statistics of heavy particles in turbulent flows, at changing both Stokes and Reynolds numbers has been presented. The main conclusions are (i) preferential concentration plays an *almost singular* role at small Stokes. Indeed, even a quite small inertia may suffice to expel particles from those turbulent regions (vortex cores) where the most intermittent and strong acceleration fluctuations would have been experienced; (ii) for small Stokes, a good quantitative agreement between the inertial particle acceleration and the conditioned fluid tracer acceleration is obtained; (iii) at large Stokes, the main effects is filtering of the velocity induced by the response Stokes times. For  $St > 1$ , the statistical properties of fluid tracers averaged over a time window of the order of  $\tau_s$  are in a quite good agreement with the inertial particle properties.

Some important questions remain open.

It is not clear how to build up a phenomenological approach that is able to describe the inertial particles acceleration as a function of both Stokes and Reynolds numbers. For example, a naive generalisation of the multifractal description, successfully used for fluid tracers (Biferale *et al.* 2004), may be insufficient. In fact, it is not straightforward to include in such models the correlation between preferential concentration and the local topological properties of the carrier flow.

The strong fluctuations of both Kolmogorov time and Kolmogorov dissipative scale are certainly the most interesting aspects which distinguish the statistics of heavy particles in turbulence from the one measured in smooth flows. The main consequence is that even identical particles, all with the same density and the same size, may experience a “local” Stokes number (defined in terms of a “local” energy dissipation, see e.g. Collins & Keswani 2004) strongly fluctuating in space and time. It would be then important to study the statistical properties conditioned to the local Stokes number.

Concerning multiparticle statistics we want to highlight that among the most important open issues there is the characterisation of clustering both at small-scales ( $r \ll \eta$ ) and in the inertial range ( $\eta \ll r \ll L$ ). The latter case is particularly relevant for  $\tau_s$  of the order of the typical inertial range time-scales. Work in this direction will be reported elsewhere.

We acknowledge useful discussions with G. Falkovich, E. Bodenschatz and Z. Warhaft. This work has been partially supported by the EU under the research training net-

work HPRN-CT-2002-00300 “Stirring and Mixing”. Numerical simulations have been performed thanks to the support of CINECA (Italy) and IDRIS (France) under the HPC-Europa project. We thank also the “Centro Ricerche e Studi Enrico Fermi” and N. Tantalo for partial numerical support.

## REFERENCES

BALKOVSKY, E. FALKOVICH, G. & FOUXON, A. 2001 Intermittent distribution of inertial particles in turbulent flows. *Phys. Rev. Lett.* **86**, 2790–2793.

BEC, J. 2003 Fractal clustering of inertial particles in random flows. *Phys. Fluids* **15**, L81–L85.

BEC, J., CELANI, A., CENCINI, M. & MUSACCHIO, S. 2005 Clustering and collisions of heavy particles in random smooth flows. *Phys. Fluids* **17**, 073301.

BEC, J., GAWEDZKI, K., HORVAI, P. 2004 Multifractal clustering in compressible flows. *Phys. Rev. Lett.* **92**, 224501.

BIFERALE, L., BOFFETTA, G., CELANI, A., DEVENISH, B.J., LANOTTE, A. & TOSCHI, F. 2004 Multifractal statistics of Lagrangian velocity and acceleration in turbulence. *Phys. Rev. Lett.* **93**, 064502.

BIFERALE, L., BOFFETTA, G., CELANI, A., LANOTTE, A. & TOSCHI, F. 2005 Particle trapping in three-dimensional fully developed turbulence. *Phys. Fluids* **17**, 021701.

BOFFETTA, G., DE LILLO, F. & GAMBA, A. 2004 Large scale inhomogeneity of inertial particles in turbulent flows. *Phys. Fluids* **16**, L20–L24.

BOIVIN, M., SIMONIN, O., SQUIRES, K.D. 1998 Direct numerical simulation of turbulence modulation by particles in isotropic turbulence. *J. Fluid Mech.* **375**, 235–263.

CHEN, S., DOOLEN, G.D., KRAICHNAN R.H. AND SHE, Z.S. 1993 On statistical correlations between velocity increments and locally averaged dissipation in homogeneous turbulence. *Phys. Fluids A* **5**, 458–463.

CHUN, J., KOCH, D.L., RANI, S., AHLUWALIA, A. & COLLINS, L.R. 2005 Clustering of aerosol particles in isotropic turbulence. *J. Fluid Mech.* **536**, 219–251.

COLLINS, LR KESWANI, A 2004 Reynolds number scaling of particle clustering in turbulent aerosols *New J. Phys.* **6**, 119.

CSANADY, G. 1980 *Turbulent diffusion in the environment*. Geophysics and Astrophysics Monographs Vol. 3 D. Reidel Publishing Company.

EATON, J.K. & FESSLER 1994 Preferential concentrations of particles by turbulence. *Int. J. Multiphase Flow* **20**, 169–209.

FALKOVICH G., FOUXON A. & STEPANOV M. 2002 Acceleration of rain initiation by cloud turbulence. *Nature* **419**, 151–154.

FALKOVICH, G. & PUMIR, A. 2004 Intermittent distribution of heavy particles in a turbulent flow. *Phys. Fluids* **16**, L47–L51.

FALKOVICH, G. 2005 Private Communication.

HILL, R.J. 2002 Scaling of acceleration in locally isotropic turbulence. *J. Fluid Mech.* **452**, 361–370.

LA PORTA, A., VOTH, G.A., CRAWFORD, A.M., ALEXANDER, J. & BODENSCHATZ E. 2001 Fluid particle accelerations in fully developed turbulence. *Nature* **409**, 1017–1019.

LA PORTA, A., VOTH, G.A., CRAWFORD, A.M., ALEXANDER, J. & BODENSCHATZ E. 2002 Measurement of particle accelerations in fully developed turbulence. *J. Fluid Mech.* **469**, 121–160.

LEWIS, D. & PEDLEY, T. 2000 Planktonic contact rates in homogeneous isotropic turbulence: Theoretical predictions and kinematic simulations. *J. Theor. Biol.* **205**, 377–408.

MAXEY, M.R. & RILEY, J. 1983 Equation of motion of a small rigid sphere in a nonuniform flow. *Phys. Fluids* **26**, 883–889.

MORDANT, N., METZ, P., MICHEL, O. & PINTON, J.-P. 2001 Measurement of Lagrangian velocity in fully developed turbulence. *Phys. Rev. Lett.* **87**, 214501.

PINSKY, M. & KHAIN, A. 1997 Turbulence effects on droplet growth and size distribution in clouds—a review. *J. Aerosol Sci.* **28**, 1177–1214.

POST, S. & ABRAHAM, J. 2002 Modeling the outcome of drop-drop collisions in Diesel sprays. *Int. J. of Multiphase Flow* **28**, 997–1019.

READE, W.C. & COLLINS, L.R. 2000 A numerical study of the particle size distribution of an aerosol undergoing turbulent coagulation. *J. Fluid Mech.* **415**, 45–64.

ROTHSCHILD, B.J. & OSBORN, T.R. 1988 Small-scale turbulence and plankton contact rates. *J. Plankton Res.* **10**, 465–474.

SAWFORD, B.L. & GUEST, F.M. 1991 Lagrangian statical simulation of the turbulent motion of heavy particles. *Boundary-Layer Meteorol.* **54**, 147–166.

SAWFORD, B.L., YEUNG, P.K., BORGAS, M.S., VEDULA, P., LA PORTA, A., CRAWFORD, A.M., BODENSCHATZ, E. 2003 Conditional and unconditional acceleration statistics in turbulence. *Phys. Fluids* **15**, 3478–3489.

SEINFELD J. 1986 *Atmospheric chemistry and physics of air pollution*. J. Wiley and Sons.

SHAW, R.A. 2003 Particle-turbulence interactions in atmospheric clouds. *Ann. Rev. Fluid Mech.* **35**, 183–227.

WARHAFT, Z., GYLASON, A. & AYYALASOMAYAJULA, S. 2005 private communication.

ZAICHIK, L.I., SIMONIN, O. & ALIPCHENKOV V.M. 2003 Two statistical models for predicting collision rates of inertial particles in homogeneous isotropic turbulence. *Phys. Fluids* **15**, 2995–3005.

ZHOU, Y., WEXLER, A. & WANG, L.-P. Modelling turbulent collision of bidisperse inertial particles. *J. Fluid Mech.* **433**, 77–104.